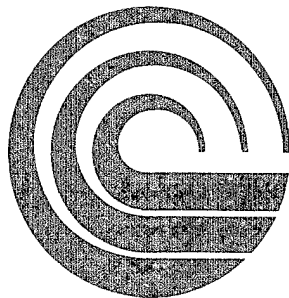


**WATER WAVES PRODUCED BY CRATERING  
EXPLOSIONS IN SHALLOW WATER**

W. J. Garcia, Jr.

October 20, 1970



**LAWRENCE  
RADIATION  
LABORATORY**  
University of California  
**LIVERMORE**

**Reproduced From  
Best Available Copy**

**DISTRIBUTION STATEMENT A**  
Approved for Public Release  
Distribution Unlimited

**20000922 112**

TID-4500, UC-35  
Nuclear Explosions—  
Peaceful Applications

**Lawrence Radiation Laboratory**  
UNIVERSITY OF CALIFORNIA  
LIVERMORE

UCRL-50940

**WATER WAVES PRODUCED BY CRATERING  
EXPLOSIONS IN SHALLOW WATER**

W. J. Garcia, Jr.

## Contents

Abstract	. . . . .	1
The Data	. . . . .	1
Analysis	. . . . .	3
Conclusions	. . . . .	5
References	. . . . .	6

# WATER WAVES PRODUCED BY CRATERING EXPLOSIONS IN SHALLOW WATER

## Abstract

In the course of developing the capability of predicting the characteristics of water waves generated by explosions detonated in shallow water beneath the ocean floor, the pertinent data from past experiments were analysed using dimensional analysis as a framework. Data were examined from one series of high explosive cratering experiments detonated beneath the floor in shallow water, and from two series of high explosive experiments and one nuclear explosive experiment detonated above the floor in shallow

water. The data indicate that the maximum radius of the water column produced by the explosion is proportional to the cube root of the ratio of explosive yield to ambient pressure at the point of detonation. Further, the data show that the maximum radius of the column of water is proportional to the square root of the product of wave height and distance from the source. The conclusions of this scheme of analysis are being tested with hydrodynamic computer code calculations.

## The Data

The data from explosion tests fired under the ocean floor in shallow water were analysed in order to gain information about the relationship between the characteristics of the water waves generated and the parameters of the explosion. Very few data are available since there have been few explosive tests of this type. All the available U.S. data are listed in Table 1.

The U.S. Army Engineer Nuclear Cratering Group conducted a series of underwater cratering tests called Project Tugboat.<sup>1,2</sup> The tests consisted of four one-ton explosions detonated at different depths of burial in the ocean floor, one 10-ton explosion, two 20-ton explosions and one 40-ton explosion, all detonated

beneath the ocean floor. The 20-ton and 40-ton explosions actually consisted of two and four charges of 10 tons each, respectively, separated horizontally by 100 to 120 ft. For the purposes of this analysis the 20-ton and 40-ton shots are assumed to be single charges. The explosive used in these tests was aluminized ammonium nitrate slurry, considered here to be equivalent in energy released to 1.62 TNT. These tests were underwater cratering experiments and were detonated in coral reef material. High speed motion pictures were taken of the test shots, and water wave measurements were made.

The Navy's Project HEAT<sup>3</sup> consisted of ten shots of two tons each fired at

Table 1. Experimental data.

Y	D	D <sub>w</sub>	R <sub>c</sub>	R	H	HR	$\frac{Y}{(D+33)^{1/3}}$	HR
Project Tugboat. Explosive: aluminized ammonium nitrate slurry (equivalent 1.62 TNT).								
1.62	15.5	4.6	47	163	2.96	483	0.322	483
1.62	19.1	5.0	50	206	1.54	317	0.314	317
1.62	23.2	5.1	50	80	4.02	321	0.306	370
				273	1.54	420		
1.62	25.8	5.0	46	161	1.97	317	0.302	306
				289	1.02	295		
16.2	42.5	6.5	98	161	11.4+	1835+	0.599	1600
				381	3.6	1370		
32.4	42	~10	—	1430	~1.5	~2140		2260
				400	4.5	1800		
				400	6.0	2400		
32.4	42	~10	—	1490	~1.5	~2240		
				290	9.0	2610		
				230	10.3+	2370+		
64.8	42	~10	—	1950	~1.5	~2920		3090
				750	4.8	3600		
				340	8.1+	2750+		
Mono Lake. Explosive: TNT.								
4.61	10.0		65	1360	0.56	751	0.475	807
				621	1.06	659		
				2160	0.47	1010		
4.62	13.8		70	4615	0.19	875	0.463	724
				2080	0.33	688		
				1170	0.52	609		
Project "Heat." Explosive: HBX-1 (equivalent 1.48 TNT).								
2.93	11.04	11.46	66.0	—	—	—	0.406	
2.92	11.74	12.00	67.5	—	—	—	0.402	
2.93	11.42	11.58	67.5	—	—	—	0.405	
2.93	4.69	9.63	62.5	—	—	—	0.426	
2.93	4.75	9.25	67.5	—	—	—	0.426	
2.92	4.96	5.04	67.5	—	—	—	0.425	
2.93	5.00	5.08	62.5	—	—	—	0.425	
2.92	4.79	5.12	62.5	—	—	—	0.425	
2.92	4.80	7.88	64.0	—	—	—	0.425	
Baker. Nuclear explosive.								
23,000	90	140	~1000	1000	94	94,000	5.72	100,000
				2000	47	94,000		
				4000	24	96,000		
				6000	16	96,000		
				8000	13	104,000		
				10000	11	110,000		
				12000	9	108,000		

Y = Explosive yield, tons TNT.

D = Depth of submergence, feet of sea water.

D<sub>w</sub> = Depth of water, feet.R<sub>c</sub><sup>w</sup> = Maximum radius of water column, feet.

R = Distance, feet.

depths varying from the ocean floor to mid-depth in the water. The explosive

used was HBX-1, assumed to be equivalent in energy released to 1.48 TNT. In these

tests, high speed motion pictures were taken to determine mound characteristics, column diameter, etc.; however, no water wave measurements were made.

At Mono Lake two explosive charges of 4.6 tons of TNT each were fired at the bottom in shallow water.<sup>4, 5</sup> Water wave measurements and measurements

of the column dimensions were made.

In addition to these few high explosive tests, Glasstone<sup>6</sup> reports the results of the Bikini test Baker, a 23 kt nuclear detonation in shallow water. He reports the measured wave heights, the range at which these measurements were made, and the approximate column radius.

## Analysis

An empirical approach was used in the analysis of the data; however, dimensional analysis provided the basic relationships among the variables involved. Two useful dimensionless products emerge:

$$\Pi_1 = \frac{L^4 \rho g}{Y}, \quad (1)$$

$$\Pi_2 = \frac{p L^3}{Y}, \quad (2)$$

where  $L$  is a characteristic length (to be specified later),  $Y$  is yield (units of energy),  $p$  is pressure,  $\rho$  is density and  $g$  is the acceleration of gravity. Since we know that the wave energy per unit area is proportional to the square of the wave height ( $H^2$ ) and the total energy is distributed over an area proportional to the square of the radius of the area of the disturbance ( $R^2$ ), we see by dimensional considerations that we can specify the characteristic length factor  $L^4$ , and can rewrite  $\Pi_1$  as

$$\Pi_1 = \frac{H^2 R^2 \rho g}{Y}. \quad (3)$$

This product (3) appears promising, since for oscillatory waves due to a

central disturbance the product  $HR$  should be constant for a given wave. We plot  $\overline{HR}$  vs the yield  $Y$  in Fig. 1; the value of  $\overline{HR}$  is the average for each wave measurement. In all cases  $H$  is the amplitude of the largest wave from crest to the following trough (in most cases this was the first wave in the train). The curves drawn show both the relationship given by Eq. (3)  $HR = C \times Y^{0.5}$  and the relationship determined by a least-squares fit of the data,  $\overline{HR} = 297 \times Y^{0.576}$ . There are insufficient data to make any conclusions concerning the merits of either relation. Figure 1 does indicate, however, that there are other factors which have subtle but significant effects, and that all the experiments examined were not completely similar.

Next we try to specify the length factor  $L^3$  in the dimensionless product  $\Pi_2$ . It is known that depth of burst plays a significant role in underwater explosions, since the maximum size to which the bubble grows is a function of the ambient pressure, hence of the depth of burst.<sup>7</sup> Also, the maximum radius of the water column,  $R_c$ , is directly related to the maximum size of the gas bubble when it

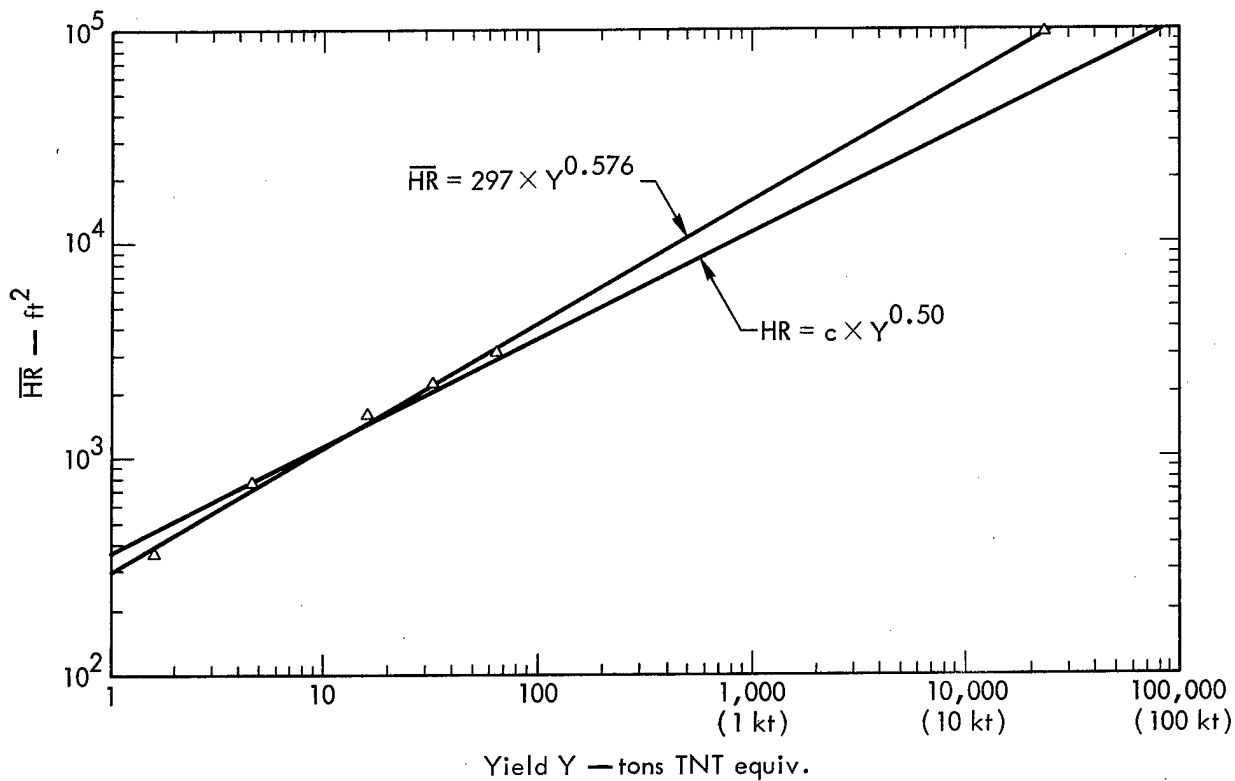


Fig. 1. Product of wave height  $\times$  distance (average for each measurement) vs yield.

reaches the surface and vents to the atmosphere. Thus  $R_c$  should be related to the yield  $Y$  and the overburden pressure  $p$ ; making this assumption leads us to rewrite  $\Pi_2$  as

$$\Pi_2 = \frac{p R_c^3}{Y} \quad (4)$$

Accordingly, Fig. 2 shows a plot of the maximum column radius vs the cube root of the ratio of yield to overburden pressure. The yield  $Y$  is expressed in tons to TNT equivalent and the overburden pressure  $p$  is expressed in feet of sea water ( $p = C \times (D+33)$ , where  $D$  is depth of submergence in feet). The available data, as can be seen, follow very closely the relation dictated by the product  $\Pi_2^{(4)}$ .

At this point it was decided to use the maximum column radius to normalize

wave height with respect to yield. A plot of the ratio of wave height to maximum column radius ( $H/R_c$ ) vs the ratio of

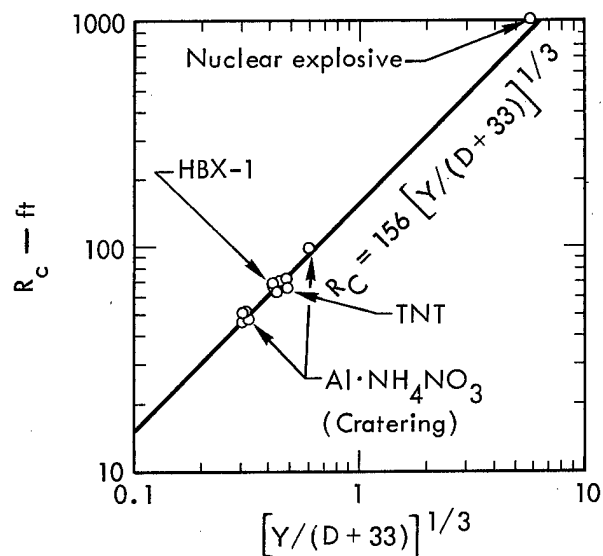


Fig. 2. Maximum radius of water column,  $R_c$ , plotted against a function of the yield  $Y$  (tons TNT equivalent) and the depth of burst  $D$  (feet).

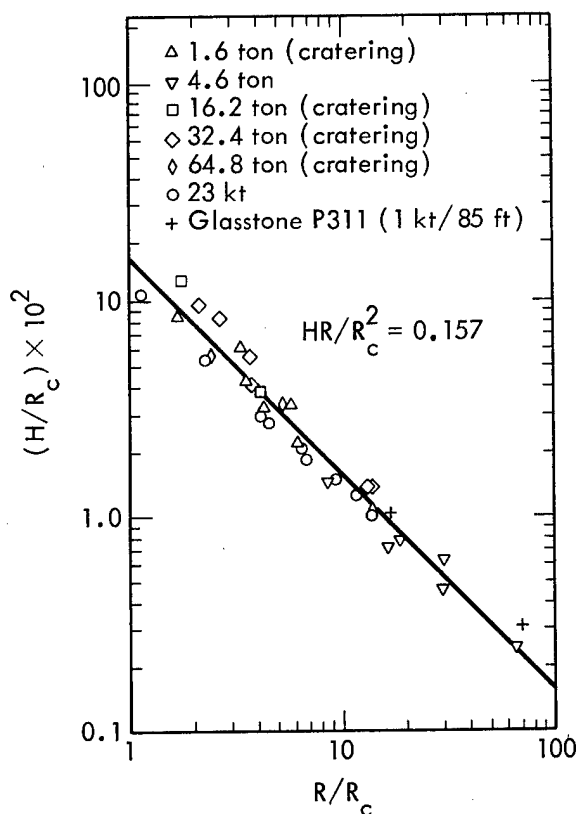


Fig. 3. Ratio of wave height to column radius ( $H/R_c$ ) plotted against ratio of distance to column radius ( $R/R_c$ ), for all available underwater explosion data.  
 $R_c = 156 \left( \frac{Y}{D+33} \right)^{1/3}$ , where  $Y$  is yield and  $D$  is depth of burst.

distance to maximum column radius ( $R/R_c$ ) is shown in Fig. 3. The available data lie within a band of two standard deviations about the best fit curve

$HR/R_c^2 = \text{constant}$ . Thus the maximum column radius  $R_c$  seems to be a good normalizing factor for eliminating the yield and over-burden pressure.

Figure 4 combines Figs. 2 and 3 plotting  $(\overline{HR})^{1/2}$  vs  $[Y/(D+33)]^{1/3}$ . The value of  $\overline{HR}$  shown is the average for each wave measurement. The average percent difference of these data from the best fit curve  $(\overline{HR})^{1/2} = 60.7 [Y/(D+33)]^{1/3}$  is 6%. The effects of changes in water depth on the wave height were not considered due to lack of data.

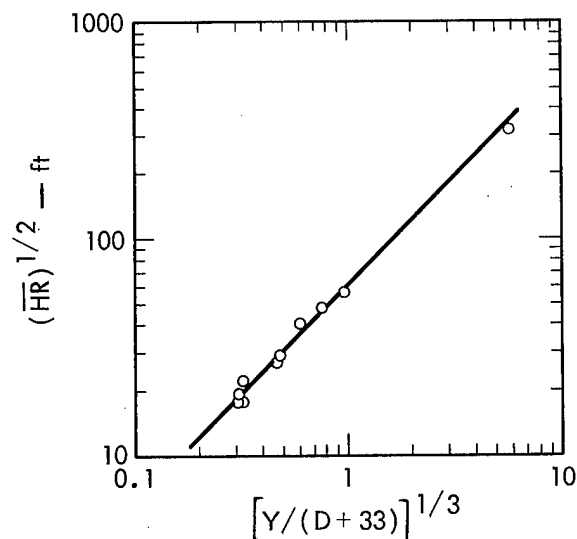


Fig. 4. Product of wave height  $\times$  distance (average for each measurement) vs function of yield  $Y$  and depth of burst  $D$ .

## Conclusions

In this paper the author has assembled all the relevant U.S. underwater test data for the water wave problem, and has found a framework for interpretation based on similitude. The prediction of water wave phenomena resulting from nuclear explosions beneath the ocean

floor may indeed be possible using this physical framework. However, hydrodynamic code calculations at intermediate to high yields are required to confirm this scheme in the absence of full-scale experimental data. Currently, calculations are being made which will permit



the modeling of underwater cratering explosions using the ABMAC hydrodynamic code as developed by Viecelli.<sup>8,9</sup> The

flexibility of this code is proving to be very valuable in the simulation of the water wave phenomenon.

## References

1. U.S. Army Engineer Nuclear Cratering Group, "Operations Plan for Project Tugboat, Phase I, Safety Calibration Series," unpublished report (1969).
2. U.S. Army Engineer Nuclear Cratering Group, "Operations Plan for Project Tugboat, Phase II, Entrance Channel and Berthing Basin Excavations," unpublished report (1970).
3. Willey, R. L. and D. E. Phillips, "Surface Phenomena Measurements and Experimental Procedures in 4000 lb. HBX-1 Shallow Underwater Explosion Tests (Project 'HEAT')," U.S. Naval Ordnance Laboratory, NOLTR 68-74 (1968).
4. Wallace, N. R., Oceanographic Services, Inc., private communication (1967).
5. Wallace, N. R. and C. W. Baird, "Runup on an Irregular Shoreline—Mono Lake Tests," Oceanographic Services, Inc., USAEC NVO-297-2 (1968).
6. Glasstone, S., The Effects of Nuclear Weapons (U.S. Atomic Energy Commission, Washington, D.C., 1962), p. 285-287.
7. Cole, Robert H., Underwater Explosions (Princeton University Press, Princeton, 1948), p. 274-275.
8. Viecelli, James A., "A Method for Including Arbitrary External Boundaries in the MAC Incompressible Fluid Computing Technique," J. Comp. Phys. 4, (4), 543-551 (1969).
9. Viecelli, James A., "Test Calculations with the ABMAC Incompressible Hydrodynamic Code," Lawrence Radiation Laboratory Report UCID-15681 (1970).

## Distribution

### LRL Internal Distribution

Michael M. May/D. Sewell

R. Batzel

A. Biehl

J. Carother

T. Cherry

P. Coyle

L. Crooks/E. Harp

D. Dorn

G. Dorough

F. Eby

E. Fleming

W. J. Garcia

E. Goldberg

J. Hadley

A. C. Haussmann

W. Harford

G. Higgins

F. Holzer

J. Kane

J. Knox

J. Kury

A. Lewis

C. McDonald

P. Moulthrop

W. Nervik

M. Nordyke

T. Perlman

D. Rabb

H. Reynolds

H. Rodean

J. Rosengren

B. Rubin

J. Shearer

B. Shore

E. Teller

J. Toman

W. Vandenberg

J. A. Viecelli

G. Werth

TID Berkeley

TID File

20

30

### External Distribution

J. S. Kelly

Division of Peaceful Nuclear

Explosives

Washington, D.C.

25

R. E. Miller

D. Thornbrough

Nevada Operations Office

Las Vegas, Nevada

5

A. R. Wilson

Australian Atomic Energy

Commission

NSW, Australia

P. Crooks

Atomic Energy Attache

Australian Embassy

Washington, D.C.

R. L. Wiegel

J. W. Johnson

P. Wilde

University of California

Berkeley, California

W. G. VanDorn

Scripps Institution of Oceanography

La Jolla, California

B. LeMehaute

Tetra Tech, Inc.

Pasadena, California

R. Y. Hudson

U.S.A.E. Waterways Experiment

Station

Vicksburg, Mississippi

A. Kamel

Louisiana State University

Baton Rouge, Louisiana

E. Peixotto

U.S.A.E. Waterways Experiment

Station

Vicksburg, Mississippi

T. Saville, Jr.

Coastal Engineering Research

Center

Washington, D.C.

W. Hoyer

ESSO Product Research

Houston, Texas

3

TID-4500 Distribution, U-35,

Nuclear Explosions—

Peaceful Applications

243

KD/lc/lp